Feedback regulation between aquatic microorganisms and the bloom-forming cyanobacterium *Microcystis aeruginosa*

Meng Zhang[1], Tao Lu[1], Hans W Paerl[2,3], Yiling Chen[4], Zhenyan Zhang[1], Zhigao Zhou[1], Haifeng Qian[1,*]

1. College of Environment, Zhejiang University of Technology, Hangzhou 310032, P.R. China;

2. Institute of Marine Sciences, University of North Carolina at Chapel Hill, Morehead City, NC, 28557, USA;

3. College of Environment, Hohai University, Nanjing, 210098, P.R. China;

4. Department of Civil, Environmental, and Geo- Engineering, University of Minnesota, Minneapolis, MN, 55455-0116, USA

Running title: Feedback between microorganisms and cyanobacterium

[*]Correspondence Author: Tel.:+86 5718832 0742, Fax: +86 571 8832 0599, E-mail address: hfqian@zjut.edu.cn (Qian H).

ABSTRACT The frequency and intensity of cyanobacterial blooms are increasing worldwide. Interactions between toxic cyanobacteria and aquatic microorganisms need to be critically evaluated to understand microbial drivers and modulators of the blooms. In this study, we applied 16S/18S rRNA gene sequencing and metabolomics analyses to measure the microbial community composition and metabolic responses of the cyanobacterium *Microcystis aeruginosa* in a coculture system receiving dissolved inorganic nitrogen and phosphorus (DIP) close to representative concentrations in Lake Taihu, China. *M. aeruginosa* secreted alkaline phosphatase using a DIP source produced by moribund and decaying microorganisms when the P source was insufficient. During this process, *M. aeruginosa* accumulated several intermediates in energy metabolism pathways to provide energy for its sustaining high growth rates, and increased intracellular sugars to enhance its competitive capacity and ability to defend itself against microbial attack. It also produced a variety of toxic substances, including microcystins, to inhibit metabolite formation via energy metabolism pathways of aquatic microorganisms, leading to a negative effect on bacterial and eukaryotic microbial richness and diversity. Overall, compared with the monoculture system, the growth of *M. aeruginosa* was accelerated in coculture, while the growth of some cooccurring microorganisms was inhibited; with the diversity and richness of eukaryotic microorganisms being more negatively impacted than prokaryotic microorganisms. These findings provide valuable information for clarifying how *M. aeruginosa* can potentially modulate its associations with other microorganisms, with ramifications for its dominance in aquatic ecosystems.

IMPORTANCE This study we measure the microbial community composition and metabolic responses of *Microcystis aeruginosa* in a microcosms coculture system receiving dissolved inorganic nitrogen and phosphorus (DIP) close to the average concentrations in Lake Taihu. In the coculture system DIP is depleted, and growth and production of aquatic microorganisms can be stressed by a lack of DIP availability. *M. aeruginosa* could accelerate its growth via interactions with specific cooccurring microorganisms, and the accumulation of several intermediates in energy metabolism-related pathways. Furthermore, *M. aeruginosa* can decrease carbohydrate metabolism of cooccurring aquatic microorganisms and thus disrupt microbial activities in the coculture. This also had a negative effect on bacterial and eukaryotic microbial richness and diversity. Microcystin was capable of decreasing the biomass of total phytoplankton in aquatic microcosms. Overall, compared with the monoculture, the growth of total aquatic microorganisms is inhibited, with the diversity and richness of eukaryotic microorganisms being more negatively impacted than prokaryotic microorganisms. The only exception is *M. aeruginosa* in the coculture system, whose growth was accelerated.

KEYWORDS *Microcystis aeruginosa*, aquatic microcosm, 16S/18S rRNA gene sequencing, metabolomics analyses, cocultures

Introduction

Anthropogenic nutrient enrichment and climatic changes, as well as exotic species invasions, can induce dramatic disturbances and regime shifts in ecosystems (1, 2). In aquatic ecosystems, the emergence of cyanobacterial harmful algal blooms (CyanoHABs) during the transition from oligotrophic to eutrophic conditions represents a regime shift, as indicated by changes in dominant microbes and new combinations of various microbial communities. CyanoHABs, especially *Microcystis* blooms, pose a major threat to freshwater ecosystems globally by altering food webs, creating hypoxic zones and producing secondary metabolites (i.e., “cyanotoxins”) that can negatively impact biota ranging from aquatic macrophytes to invertebrates, fish and mammals, including humans (3, 4).

Cyanobacteria are among the most ancient living organisms on Earth (~3 billion years ago). Their diverse and flexible metabolic capabilities enable them to adapt to major environmental changes (3). Essential nutrients such as nitrogen (N) and phosphorus (P) play key roles in supporting cyanobacterial production and composition in freshwater systems (5, 6). However, excessive inputs of nutrients can promote the development and proliferation of CyanoHABs (3, 7), especially with increasing water temperature (8). The frequency, intensity and duration of cyanobacterial blooms in many aquatic ecosystems globally are linked to accelerating eutrophication. Recent studies have shown that reductions of both P and N inputs is essential for controlling blooms (9, 10, 11, 12). Moreover, studies have shown that *Microcystis* is capable of scavenging dissolved organic phosphorus (DOP), thereby

providing a source of P under dissolved inorganic phosphorus (DIP) deplete conditions (6).

Secondary metabolites produced by *Microcystis* (microcystins (MCs), micropeptins, linoleic acid, etc.) have been shown to be toxic to some biota (13, 14, 15). For example, *Microcystis* is capable of inhibiting photosynthesis, carbon metabolism and amino acid metabolism in *Chlorella pyrenoidosa* via the production of linoleic acid (16). Additionally, the microbial community associated with CyanoHABs is different from that under non-bloom conditions (17, 18). *Microcystis* blooms strongly affect eukaryotic abundance (13, 17). Field studies in Lake Taihu, the 3rd largest freshwater lake in China, have shown that blooms had a negative effect on bacterial diversity and richness (19, 20). Zooplankton (including crustaceans, rotifers and protozoa) have a limited ability to ingest cyanobacteria, especially colonial and filamentous genera; Meanwhile, some cyanobacterial secondary metabolites can also be toxic to zooplankton. These constraints can negatively impact transfer of cyanobacterial biomass to higher trophic levels (21, 22). Furthermore, some cyanobacterial genera can fix atmospheric N, thereby providing biologically-available N on the ecosystem-scale (23). Some bacteria attach to cyanobacterial cells, and they can grow on extracellular mucus or form free-living populations (24, 25). Overall, there is renewed interest in how *M. aeruginosa* and aquatic microorganisms interact under varying nutritional conditions.

In this study, we utilized a laboratory coculture system, in which a dialysis membrane was used to separate *M. aeruginosa* and aquatic microorganisms in a microcosm,

Applied and Environmental Microbiology

allowing their growth in an isolated culture and exchange of excretion products. The system allowed for measurements of physicochemical water quality parameters (detailed in Material and Methods), cell enumeration, microbial composition and diversity (high-throughput sequencing data sets, including 16S and 18S rRNA gene sequencing) and metabolomics analysis to address the interactions between *M. aeruginosa* and the native microbial community.

RESULTS AND DISCUSSION

***M. aeruginosa* and microbial growth states.** According to Figure 1B, OD_{680} and the amount of *M. aeruginosa* cells in the Treat-Ma group were significantly higher than those in the Con-Ma group after 3 d of coculture. However, OD_{680} and Chl-a levels in the Treat-AM group were significantly lower than those in the Con-AM group (Figure 1C). Figure S2 also showed that the turbidity of the medium changed in coculture microcosms (more transparent) compared to that of Con-AM after 8 d of culture, indicating that the growth of cooccurring microorganisms was inhibited in the coculture system.

In addition, DO and pH values were significantly lower during the coculture process in the Treat-AM group than in the Con-AM group (Figure 2). Dense *Microcystis* populations can consume oxygen through respiration at night and through microbial decomposition of moribund cells, resulting in an insufficient oxygen supply in the water to support aerobic microbes and higher organisms (26, 27). An increase in the concentration of carbon dioxide shifts the inorganic carbon equilibrium away from

carbonate towards bicarbonate, decreaing pH, which in turn inhibits the growth of some microbial populations (28). Furthermore, *Microcystis* inhibited some microorganisms and the decomposition of these moribund cells would lead to an increase in oxygen consumption in the Treat-AM group (Figure 2D). The EC of each group was investigated as a function of the types and quantities of dissolved materials (29). Compared with the Con-AM group, the Treat-AM group showed an apparent increase in EC after 3 and 6 d of coculture. Notably, these water quality parameters (Figure 2, especially pH value) were significantly different between monoculture and coculture systems, suggesting that these physiochemical changes in the water were influenced by the metabolism of *M. aeruginosa* directly or indirectly, and by the associated microbial community.

Changes in N and P and MCs released in culture medium. Nitrogen and phosphorus availability are key factors controlling primary production and CyanoHABs dynamics (12). In this study, the concentrations of TP and DIP in coculture medium were lower than those in monoculture medium after 1 and 2 d of coculture, while the concentrations of TP and DIP in coculture medium were higher than those in monoculture medium after 3-8 d of coculture (Figure 3A). Numerous algal species can synthesize AKP to hydrolyze DOP to DIP when TP is too low in order to satisfy algal growth demand (6). Consistent with previous studies (30), AKP in the Treat-Ma group increased dramatically on 2 and 4 d of coculture, while AKP decreased with an increase in DIP (Figure 3C). These results suggest a strong ability of *M. aeruginosa* to scavenge DOP from metabolic products released by organisms

144 (6). With the active growth of *M. aeruginosa*, the NO_3^--N level in coculture system
145 was also much higher than that in the monoculture system (Figure 3B). This was due
146 to the negative effect of *M. aeruginosa* on the growth of some accompanying species
147 in the cocultured systems, leading to the release of nitrogen sources from moribund
148 cells, while the reduction of aquatic microorganisms also decreases the consumption
149 of nitrogen sources. This released N provided a readily available N source for *M.*
150 *aeruginosa* growth, which might partly explain why *M. aeruginosa* growth in
151 coculture is better than that in monoculture. There are likely multiple reasons why
152 *Microcystis* growth is better in coculture, including exchange of mutually-beneficial
153 metabolites, like vitamins, CO_2 replenishment, exchange of nutrients and essential
154 metals (31).

155 During coculture, *M. aeruginosa* exhibited more rapid growth relative to
156 monocultures and produced a large number of MCs that were released into the culture
157 medium. After 3 d of coculture, the MCs in Treat-AMW were significantly higher
158 than those in Con-AMW (Figure 3D). Numerous studies have shown that MCs are
159 toxic to some microorganisms (32). Our data also indicated that MCs caused a
160 decrease in total phytoplankton in aquatic microcosms, as shown in Figure 7a.

161

162 **Changes in bacterial community structure and diversity in aquatic microcosms**
163 **under coculture conditions.** Community diversity analysis was calculated based on
164 the OTU level. The Shannon and Simpson indices reflect the diversity and evenness
165 of the community. Meanwhile, the ACE and Chao1 indices reflect the richness, which

indicates the estimated number of species present (33). Compared with the Con-AM group, the Treat-AM group showed a downward trend in the ACE and Chao1 indices at 4 and 8 d, and the Shannon and Simpson diversity indices also slightly decreased at 8 d in the Treat-AM group (Table 1), indicating a decline in the richness and diversity of bacterial communities. Observed species in Table 1 indicates the number of species contained in the sample. Higher values of observed species in the Con-AM group also indicated higher species richness than in the Treat-AM group. Changes in dominant cyanobacterial biomass affect the composition and function of microbial populations, while competitive exclusion tends to reduce the abundance of other, more readily grazed primary producers during cyanobacterial blooms (3, 4). Principal component analysis (PCoA) showed that PC1 (first principal component) and PC2 (second principal component) explained 83.89% of the β-diversity (Figure 4A) in the variation of species composition on the temporal scales. Coculture treatment could constitute a major portion of PC1, as it might result in the separation of the Con-AM and Treat-AM samples after 4 and 8 d of culture. Environmental factors such as nutritional status, pH and predation might constitute PC2, which affects the OTU composition at certain times in culture (from 4 d to 8 d). As shown in Figure 4B, the eigenvalues of the first two RDA axes explained 67.42% of the total variation. The RDA scores showed strong relationships between the environmental variables and the four groups. Samples of Con-AM4 and Con-AM8 were positively correlated with EC, DO, pH and NO_3^--N. Treat-AM8 and Treat-AM8 clustered together and showed the highest correlation with MCs and DIP.

188 Bacterial community analysis revealed that the microbial community in the
189 microcosms at the class level was dominated by *Cyanobacteria*, *Alphaproteobacteria*,
190 *Betaproteobacteria* and *Sphingobacteria* in both 4 and 8 d coculture and monoculture
191 (Figure 4C), while other classes did not exceed 1%. In both cocultures and
192 monocultures, *Cyanobacteria* (>50%) was the dominant class of abundance, and the
193 top four genera of abundance among the *Cyanobacteria* were *Pseudanabaena*,
194 *Merismopedia*, *Limnothrix* and *Arthronema gygaxiana UTCC 393* in aquatic
195 microcosms on 4 d and 8 d (Figure 4D). Interestingly, the abundance of
196 *Cyanobacteria* in the aquatic microcosms was significantly lower in the Treat-AM8
197 group than in the Con-AM8 group, except for *Pseudanabaena*. The growth of some
198 freshwater bacteria has been reported to be associated with cyanobacterial blooms, but
199 phytoplankton species are mainly conserved at the phylum level in *Proteobacteria*,
200 *Bacteroidetes* and *Actinobacteria* (34). After coculture with *M. aeruginosa*,
201 *Alphaproteobacteria* and *Betaproteobacteria* significantly increased, while
202 *Sphingobacteria* decreased, indicating that the abundance of some bacteria was
203 affected by an increase in *M. aeruginosa* biomass. Moreover, coculture with *M.*
204 *aeruginosa* disturbed the composition of rare microorganisms (relative abundance <
205 1%). Hundreds of rare microorganisms decreased in relative abundance or
206 disappeared after 8 d in coculture (Dataset 1).
207
208 **Changes in eukaryotic microorganism community structure and diversity in**
209 **aquatic microcosms cocultured with *M. aeruginosa*.** The decrease in species

diversity and richness from the Con-AM4 to Con-AM8 group indicated a decline in eukaryotes over time (Table 2). The species diversity and richness from the Treat-AM group at 4 to 8 d did not show a downward trend; however, compared with the Con-AM group, the Treat-AM group at 4 and 8 d showed a downward trend in both the ACE and Chao1 indices of eukaryotic microorganisms and the Shannon and Simpson diversity indices. These findings indicate that coculture reduces the diversity and richness of eukaryotic species. PCoA analysis showed that PC1 and PC2 explained 92.03% of the β-diversity (Figure 5A). The coordinates of the Con-AM4 and Treat-AM4 groups were separated by PC1, and the Con-AM8 and Treat-AM8 groups were affected more severely by PC2. Changes in the 4 d cocultures may be affected by *M. aeruginosa*, and the changes physicochemical water quality parameters, such as pH and dissolved oxygen, may be related to 8 d cocultures.

In the eukaryotic community, diverse species were identified, including some chromista such as *Ciliophora* and *Ochrophyta*; metazoans such as *Rotifera*; viridiplantae such as *Streptophyta*, and fungi such as *Cryptomycota*, *Ascomycota* and *Dikarya* (Figure 5B). There are interrelationships between eukaryotes in areas such as predation, competitive relationships, and parasitism (25). In monocultures, *Rotifera* was the most abundant eukaryote, accounting for 29.88% and 43.81% of the eukaryotic sequences of the Con-AM group. Rotifers are usually very active grazers affecting phytoplankton biomass and richness in the Con-AM group. Compared with the Con-AM group, the Treat-AM group showed a reduction in the relative abundance of *Rotifera* to 8.00% and 23.45% after 4 and 8 d of coculture, respectively, and

Ciliophora became the most abundant eukaryote in cocultures. As consumers, *Rotifera and Ciliophora* are correlated in predation and nutrition competition experiments (35). Our study showed that toxic blooms have greater impacts on the composition of these active grazers and therefore change their food (aquatic microorganism) items. In contrast, other eukaryotes such as *Cryptomycota*, *Streptophyta*, *Ascomycota* and *Chordata* decreased after coculture. Additionally, rare microorganisms moved closer to the coordinate axis in the Treat-AM4 and Treat-AM8 groups compared with those in the Con-AM4 and Con-AM8 groups, suggesting the decrease or complete disappearance of the rare microorganisms (Figure 5C). The synergistic effects between rare and common taxa may play central roles in maintaining the stability of the eukaryotic community and its ecological function (36).

Metabolic responses of *M. aeruginosa* and aquatic microcosms in cocultures and monocultures. To clarify the mechanisms underlying the effect of *M. aeruginosa* on the microcosm community, we measured metabolite changes in *M. aeruginosa* and microcosms. A total of 239 metabolites were identified. The score plot of PCA and PLS-DA showed noticeable separation between cocultures and monocultures from *M. aeruginosa* and the microcosm along PC1 (Figure 6A and Figure S3). In multivariate statistical analysis, screening and determining the difference variables were performed by calculating the variable importance (VIP) between groups. VIP is the weighted sum of squares of the PLS-DA analysis, which indicates the importance of a variable to the entire model (37). A variable with a VIP greater than 1 is regarded as

254 responsible for separation, defined as a discriminating metabolite in this study. In a
255 univariate statistical analysis, the *p* value was used to assess the statistical significance
256 of difference variables. We combined these two criteria to screen variables with VIP >
257 1 and *p* value < 0.05 as difference variables. Significant metabolite changes were
258 observed for *M. aeruginosa* (53 downregulated and 31 upregulated in Table S2),
259 aquatic microorganisms from microcosms (39 downregulated and 18 upregulated in
260 Figure S4), and culture medium samples (53 downregulated in Table S3 and 10
261 upregulated in Table 3), respectively.
262
263 **Metabolic profiles and pathway changes in *M. aeruginosa* and aquatic**
264 **microcosms in cocultures and monocultures.** The components of the pentose
265 phosphate (PP) pathway or glycolysis intermediates, such as glucose-6-phosphate
266 (G6P), fructose-6-phosphate (F6P) and ribulose-5-phosphate (Ru5P), significantly
267 increased in Treat-Ma (Figure 6B) relative to Con-Ma. G6P and F6P are
268 interconnected through biochemical reactions with Calvin cycle, to glycogen
269 biosynthesis for energy expenditure (38, 39). Their accumulation played an active role
270 in the growth of *M. aeruginosa*, which indicated that the carbon fixation in *M.*
271 *aeruginosa* cells was enhanced by the co-culture treatment. Succinic acid, an
272 intermediate in the tricarboxylic acid (TCA) cycle, was 18.30-fold higher in the
273 Treat-Ma group than in the Con-Ma group. These increased intermediates in PP
274 pathway, glycolysis and TCA cycle could provide precursors for amino acid synthesis
275 and transfer of other cellular macromolecules (40, 41). They are also beneficial in the

276 generation of reducing power (NADPH and NADH) and energy (ATP) for AKP and
277 MC synthesis and cell growth. The AKP synthesis in *M. aeruginosa* implied the
278 manifestation of cellular responses to stress (6), specifically the hydrolysis of DOP to
279 support *M. aeruginosa* growth under low DIP conditions. Higher metabolite levels
280 accelerated *M. aeruginosa* growth, forming aggregates that are dominant in
281 competition with microbes, and produce various toxic substances that inhibit the
282 growth of other microbes. This conclusion is illustrated in Figures 1B and 3D, where
283 the growth of *M. aeruginosa* in the coculture system was faster than that in
284 monoculture and a large amount of MCs was produced. Overall, the upregulation of
285 these pathways in *M. aeruginosa* was beneficial for the production of MCs, AKP and
286 energy, thus enhancing the competitive capacity and defensive ability of *M.*
287 *aeruginosa*.

288 Sugars participate in energy metabolism, play critical roles as signaling
289 molecules (42) or as osmoprotectants (43). A significant increase of compatible solute
290 ($p \leq 0.05$) in coculture, such as tagatose, 1,5-anhydroglucitol, sucrose and allose in the
291 Treat-Ma group, decreased the water potential inside the cells to maintain osmotic
292 pressure to avoid dehydration, as in the salt stress (43).

293 Compared to monoculture, coculture decreased the levels of several fatty acids in
294 *M. aeruginosa*, such as 1-monopalmitin (0.76-fold), stearic acid (0.63-fold), palmitic
295 acid (0.60-fold) and arachidonic acid (0.51-fold). Fatty acids and sterols with
296 phospholipids are the primary components of the plasma membrane (44).
297 Phospholipids are composed of polar head groups, glycerides, and two fatty acyl

298 chains. Glycerol metabolism, which is related to the polar head-group component of
299 phospholipid, significantly ($p \leq 0.05$) increased upon exposure to coculture. These
300 findings support the hypothesis that *M. aeruginosa* adjusts its membrane composition
301 to maintain membrane integrity, and an increase in the cell division of *M. aeruginosa*
302 alters intracellular metabolism to rebuild membrane integrity.

303 Amino acids play important roles in cyanobacterial physiological processes by
304 acting as osmolytes, serving as precursors for the synthesis of defense-related
305 metabolites and signaling molecules (45). Therefore, it contributed to a holistic
306 understanding of cyanobacteria against stress (46). A number of amino acids,
307 including hydroxylamine (0.71-fold), norleucine (0.83-fold), N-methyl-DL-alanine
308 (0.71-fold), and alanine (0.72-fold), were lower in the Treat-Ma group than in the
309 Con-Ma group. We postulated that the decrease in amino acids (containing N
310 elements) in the Treat-Ma group was caused by the acceleration of protein synthesis
311 to satisfy the growth of *M. aeruginosa*. Aspartate can be synthesized by
312 microorganisms via TCA cycle intermediates, which is an important substrate for
313 microcystin biosynthesis in *M. aeruginosa* (47, 48). An increase in aspartate in
314 Treat-Ma may contribute to the over-production of microcystin (Figure 3D).

315 In microcosms, several intermediates involved in energy metabolism pathways,
316 such as glycolysis, TCA cycle and sugar metabolism, decreased after coculture in the
317 Treat-AM group (Figure 6C). The reduction of these intermediates could be attributed
318 to the reduced defensive ability of aquatic microorganisms caused by negative
319 environmental factors (pH, DO, MCs, DIP). This finding is also consistent with the

decrease in Chl-a in the aquatic microcosm after coculture.

Interspecies network of interactions. At the metabolomics level, the contents of the following metabolites particularly increased in the Treat-AM group: d-glyceric acid (1.78-fold), monoolein (1.63-fold) and diglycerol (1.63-fold; Table S2). Furthermore, the concentrations of monoolein, d-glyceric acid, diglycerol and MCs (independently analyzed by a beacon MC plate kit) in coculture medium were higher than those in monoculture medium (Table 3), demonstrating that these compounds were secreted by *M. aeruginosa*. Monoolein is nontoxic and biodegradable, while diglycerol can be bioavailable as a carbon source (49, 50). To verify their potential allelopathic roles, MCs and d-glyceric acid were added into separate monoculture microcosms. The Chl-a content decreased with the presence of MCs in aquatic microcosms but remained constant with glycerate acid (Figure 7), implying that MCs play a role in the decrease in total phytoplankton in microcosms. We were unable to verify whether MCs could change the original cultured microbial community. However, MCs caused a decrease in total phytoplankton in microcosms. MCs appear to be toxic to some nearby organisms, and the binding of MCs may protect cyanobacterial proteins from oxidative stress to enhance the viability of cyanobacteria (27, 51). In addition to the upregulation of metabolites, the downregulation of various substances (such as glucose-1-phosphate, malonic acid, carnitine) metabolized by *M. aeruginosa* or aquatic microorganisms was more obvious in coculture medium (Treat-AMW/Con-AMW $\leq$ 0.28, Table S3). The downregulation of these substances

may also affect the growth of aquatic microorganisms in cocultures compared to that in monocultures.

A schematic diagram of changes in *M. aeruginosa* and microbial communities after coculture treatment is shown in Figure 8. Our study demonstrated that *M. aeruginosa* can secrete AKP, making DOP produced by dying and decaying microorganisms available when the P source is insufficient. At the same time, *M. aeruginosa* produces a variety of toxic substances such as MCs, inhibiting some key intermediates accumulating in energy metabolism pathways (such as glycolysis, TCA cycle and sugar metabolism) in aquatic microorganisms and thus inhibiting microbial growth. *M. aeruginosa* produced MCs, AKP and energy to enhance its competitive capacity and defensive ability during its growth. *M. aeruginosa* slightly decreased bacterial microbial community diversity and abundance but had a more significant impact on the diversity and abundance of eukaryotes. Furthermore, some metabolites released from *M. aeruginosa* or from *M. aeruginosa* lysis could be harmful to biota and negatively affect the growth of algal competitors or predators, which could be the key factor to enable this opportunistic group of photosynthetic prokaryotes to thrive in a wide range of habitats.

MATERIALS AND METHODS

Aquatic microcosms and *M. aeruginosa* culture. Water samples were collected in sterile containers during the bloom-free phase from Meiliang Bay on Lake Taihu (30°55′40″-31°32′58″N; 119°52′32″-120°36′10″ E), a location where the water quality

364 is monitored monthly, in Nov. 2017. Microorganisms first isolated from lake Taihu
365 received sterile BG-11 nutrient medium (initial pH = 7.1, chemical composition in
366 Table S1) (28). An axenic culture of *M. aeruginosa* (strain FACHB-905) obtained
367 from the Institute of Hydrobiology (Chinese Academy of Sciences, Wuhan, China),
368 was also grown on sterilized BG-11 liquid medium. All cultures were incubated in an
369 environmental chamber at 25 ± 0.5 °C under cool-white fluorescent illumination (46
370 μmol /m^2/s, 12 h light/12 h dark).
371
372 **Coculture experimental design.** A coculture design was used to investigate the
373 interactions between axenic *M. aeruginosa* and aquatic microorganisms. Sterile
374 permeable dialysis cellulose membrane tubing (Economical Biotech Membrane, 14
375 KD, 77 mm Width; Sangon Biotech, Shanghai, China) was used to isolate *M.*
376 *aeruginosa* and lake water microbial communities from each other. This design
377 allowed for the exudation of small molecule compounds through the dialysis
378 membrane, and prevented cell contact between *M. aeruginosa* and naturally occurring
379 microbial populations (52).
380 Prior to incubation, both microorganisms and *M. aeruginosa* (which reached
381 approximately 10^7 cells/mL) were harvested by centrifugation (8,000 g for 10 min,
382 4 °C) and washed several times with ultrapure water. The microorganisms and *M.*
383 *aeruginosa* were cultured in modified BG11 ($NaNO_3$: 10 mg/L, K_2HPO_4: 1 mg/L) for
384 1 d to allow them to adapt to experimental conditions, in which nitrate nitrogen
385 (NO_3^--N) and DIP were added at concentrations representative of ambient Lake Taihu

386 water. Three groups of experiments were carried out to observe the growth of *M.*
387 *aeruginosa* and associated aquatic microorganisms: (1) the coculture group: an axenic
388 dialysis bag filled with 180 mL of *M. aeruginosa* (Treat-Ma) was submerged in 900
389 mL of aquatic microorganisms (Treat-AM) and cocultured in a sterilized 2000-mL
390 glass beaker; (2) control group 1: a dialysis bag filled with 180 mL of *M. aeruginosa*
391 (*M. aeruginosa* control group, Con-Ma) was submerged in 900 mL of *M.*
392 *aeruginosa*-containing medium. Because 900 mL of aquatic microorganisms were
393 added outside of the dialysis bag in the coculture group, in order to maintain the
394 culturing conditions consistent with the coculture group, 900 mL of *M. aeruginosa*
395 was also added to submerge the dialysis bag in the monoculture group. Samples for
396 analysis were collected only from the 180-mL dialysis bag; (3) control group 2:
397 similar to the control 1, a dialysis bag filled with 180 mL of aquatic
398 microorganism-containing medium was submerged in 900 mL of aquatic
399 microorganisms (aquatic microorganisms control group, Con-AM).

400 The initial cell density was calculated by optical density at 680 nm (OD_{680}). For
401 the microcosm, OD_{680} was selected as 0.03, which was similar to the value of water
402 samples collected from Lake Taihu. For *M. aeruginosa*, preliminary experiments were
403 conducted with OD_{680} at 0.03, 0.06 and 0.09 (approximately 1.72×10^5 cells/mL,
404 3.44×10^5 cells/mL and 5.16×10^5 cells/mL, respectively), which were within the same
405 order of cell densities measured in Lake Taihu during water bloom phase (13). The
406 results showed that the similar inhibitory effects of *M. aeruginosa* on aquatic
407 microorganisms among the 0.03, 0.06 and 0.09 OD_{680} groups were statistically

significant (Figure S1). Therefore, the OD_{680} of both *M. aeruginosa* and the microcosm were selected as 0.03. The entire experimental process is shown in Figure 1A.

Measurements of *M. aeruginosa* and microbial growth and physicochemical water quality parameters. The growth status of *M. aeruginosa* and associated microorganisms was monitored daily by spectrophotometry. In addition, the cell density of *M. aeruginosa* was measured by cell counting, while the concentration of Chl-a represented total phytoplankton biomass in the microcosm (2). During coculture, the cell number and OD_{680} of *M. aeruginosa* and chlorophyll a (Chl-a) and OD_{680} of the microcosm were measured every 24 h. The initially cultured *M. aeruginosa* was enumerated microscopically to establish a linear regression equation between the number of cells ($y \times 10^5$ cells/mL) and OD_{680} (x). The number of cells was calculated based on the equation $y = 34.1x + 0.7$ ($R^2 = 99.17$). A series of water quality parameters was measured as follows: pH was measured using a pH meter (FE-20, Mettler Toledo®, Columbus, Ohio, USA). Electrical conductivity (EC) was measured using an EC meter (InPro 7100i/12/120, Mettler Toledo®, Zurich, Switzerland). Dissolved oxygen (DO) was measured using a DO meter (Visiferm DO120, Hamilton Bonaduz, Zurich, Switzerland). NO_3^--N, total phosphorus (TP), and DIP were measured by ultraviolet spectrophotometry, ammonium molybdate spectrophotometry and molybdenum rhenium spectrophotometry, respectively (53, 54). Alkaline phosphatase (AKP) assays were performed using a commercial kit (Suzhou Comin

Biotechology Co., Ltd, Suzhou, China). AKP can hydrolyze a natural phospholipid monoester complex and catalyze the formation of free phenol from sodium phenyl phosphate. Phenol reacted with 4-aminoantipyrine and potassium ferricyanide to form derivatives with characteristic light absorption at 510 nm.

DNA extraction, amplification and sequencing, and microbial diversity analysis. At 4 d and 8 d of incubation culture, samples were collected from control (Con-AM4 and Con-AM8, respectively) and coculture microcosms (Treat-AM4 and Treat-AM8, respectively) for DNA extraction using a MoBio PowerSoil DNA Isolation Kit (Mo Bio Laboratories Inc., Carlsbad, USA). Extracted DNA was used for Illumina 16S rRNA/18S rRNA gene amplicon sequencing. The V3-V4 region of the 16S rRNA gene was amplified using primers 341F (CCTAYGGGRBGCASCAG) and 806R (GGACTACNNGGGTATCTAAT), and the V4 region of the 18S rRNA gene was amplified using the primers 528F (GCGGTAATTCCAGCTCCAA) and 706R (AATCCRAGAATTTCACCTCT). Each group was amplified in triplicate. All PCRs were carried out with Phusion® High-Fidelity PCR Master Mix (Basel, Switzerland). Sequencing libraries were generated using TruSeq® DNA PCR-Free Sample Preparation Kit (Illumina, San Diego, USA) following the manufacturer's recommendations, and index codes were added. The library quality was assessed on the Qubit@ 2.0 Fluorometer (Thermo-Fisher Scientific, Carlsbad, USA) and Agilent Bioanalyzer (Agilent 2100, Palo Alto, USA). Lastly, the library was sequenced on the Illumina HiSeq2500 platform (Illumina, Inc., San Diego, USA), and 250-bp

paired-end reads were generated. Microbial diversity was computed using QIIME (vision 1.6.0). Operational taxonomic units (OTU: number of species normalized to the abundance of 16S rRNA/18S rRNA gene) were computed for each treatment. The OTUs in samples were aligned with the SILVA database to classify the microbial community into phylotypes.

Metabolomic analyses. At 8 d of incubation, approximately 0.3 g of *M. aeruginosa* (Con-Ma and Treat-Ma), microorganism samples (Con-AM and Treat-AM) and culture medium (Con-AMW and Treat-AMW) were collected from coculture and monoculture systems for metabolomic analysis. *M. aeruginosa* or microorganism samples were transferred to a 4-mL glass bottle with 20 μL of internal standard (2-chloro-l-phenylalanine dissolved in methanol) and 600 μL of a mixture of methanol and water (4/1, vol/vol). Chloroform (200 μL) was added before ultrasonic homogenization in an ice bath (500 W, 6 min, 6 s on, 4 s off). Samples were then centrifuged at 10,000 g. for 15 min, and supernatants were collected for further purification. The culture medium was filtered on 0.7-μm porosity Whatman GF/F fiberglass filters at 0.1 MPa, and the filtrates were collected for metabolomic analysis. The supernatant (600 μL) in a glass vial was dried in a centrifugal concentrating freeze dryer, followed by the addition of 80 μL of pyridine (containing 15 mg/mL methoxyamine hydrochloride). The resultant mixture was vortexed vigorously for 2 min and incubated at 37 °C for 90 min. BSTFA (80 μL, with 1% TMCS) and 20 μL of n-hexane were added into the mixture, vortexed vigorously for 2 min and then derivatized at 70 °C for 60 min. The derivatized samples were analyzed on an Agilent

474 7890A gas chromatograph coupled to an Agilent 5975C MSD system (Agilent, Palo
475 Alto, USA). An HP-5MS fused-silica capillary column (30 m × 0.25 mm × 0.25 μm,
476 Agilent J &W Scientific, Palo Alto, USA) was utilized to separate the derivative.
477 Finally, all MS data were analyzed using ChromaTOF software (v 4.34, LECO, St
478 Joseph, MI, USA).

479 **Quantification of MCs in culture medium.** To measure MCs in the medium,
480 water was collected from aquatic microcosms in 1.5-mL tubes and centrifuged at
481 10,000 g for 10 min at 4 °C. Then, the supernatants were used to assay MC content
482 using a beacon MC plate kit according to the manufacturer's instructions (Beijing
483 Ease Century Trade Co., Ltd, Beijing, China). The Beacon Microcystin Plate Kit uses
484 a polyclonal antibody that binds both microcystins and a microcystin-enzyme
485 conjugate for a limited number of antibody binding sites, which however, cannot
486 differentiate between MC-LR and other MC variants.

487 **Statistical analyses.** Statistical significance among data for the biochemical and
488 physiological measurements was tested with one-way ANOVAs (StatView 5.0)
489 (Statistical Analysis Systems Institute, Cary, NC, USA). Differences were considered
490 statistically significant when $p < 0.05$. Metabolomics data sets were normalized to the
491 total peak area of each sample in Excel 2007 (Microsoft, USA) and imported into a
492 SIMCA (version 14.0, Umetrics, Umeå, Sweden). Each sample was taken from
493 different cultures. Metabolomics analysis was set up in six replicates, and the
494 remaining experiments were set up in triplicate. All samples were taken at

approximately 9 am. Data was presented as the mean ± standard error of the mean (SEM).

Data availability. The 16S and 18S rRNA gene sequence data generated in this study have been deposited and are available in the NCBI Sequence Read Archive (SRA) with accession numbers SAMN12388980- SAMN12388991 (16S), and SAMN12394199- SAMN12394210 (18S).

ACKNOWLEDGEMENTS

This work was financially supported by the National Natural Science Foundation of China (21777144, 21577128) and the USA National Science Foundation, Dimensions in Microbial Diversity Program (1831096).

507 **References**

508 1. Scheffer, M., Carpenter, S., Foley, J.A., Folke, C., Walker, B., 2001. Catastrophic
509 shifts in ecosystems. Nature 413, 591-596.
510 2. Pace, M.L., Batt, R.D., Buelo, C.D., Carpenter, S.R., Cole, J.J., Kurtzweil, J.T.,
511 Wilkinson, G.M., 2017. Reversal of a cyanobacterial bloom in response to early
512 warnings. Proceedings of the National Academy of Sciences USA 114, 352-357.
513 3. Paerl, H.W., Otten, T.G., 2013. Harmful cyanobacterial blooms: causes,
514 consequences, and controls. Microbial Ecology 65, 995-1010.
515 4. Otten, T.G., Paerl, H.W., Dreher, T.W., Kimmerer, W.J., Parker, A.E., 2017. The
516 molecular ecology of *Microcystis sp.* blooms in the San Francisco estuary.
517 Environmental Microbiology 19, 3619-3637.
518 5. Paerl, H.W., 2008. Nutrient and other environmental controls of harmful
519 cyanobacterial blooms along the fresh water marine continuum. Advances in
520 Experimental Medicine and Biology 619, 217-237.
521 6. Ren, L., Wang, P., Wang, C., Chen, J., Hou, J., Qian, J., 2017. Algal growth and
522 utilization of phosphorus studied by combined monocultures and co-culture
523 experiments. Environmental Pollution 220, 274-285.
524 7. Paerl, H.W., Xu, H., McCarthy, M.J., Zhu, G., Qin, B., Li, Y., Gardner, W.S., 2011.
525 Controlling harmful cyanobacterial blooms in a hyper-eutrophic lake (Lake
526 Taihu, China): the need for a dual nutrient (N & P) management strategy. Water
527 Research 45, 1973-1983.
528 8. Paerl, H.W., Huisman. J., 2008. Blooms like it hot. Science 320, 57-58.
529 9. Lewis, W.M., Wurtsbaugh, W.A., Paerl, H.W., 2011. Rationale for control of

anthropogenic nitrogen and phosphorus to reduce eutrophication of inland waters. Environmental Science & Technology 45, 10300-10305.

10. Saxton, M.A., Arnold, R.J., Bourbonniere, R.A., McKay, R.M., Wilhelm, S.W., 2012. Plasticity of total and intracellular phosphorus quotas in *Microcystis aeruginosa* cultures and Lake Erie algal assemblages. Frontiers in Microbiology 3, 3-11.

11. Harke, M.J., Davis, T.W., Watson, S.B., Gobler, C.J., 2016. Nutrient-controlled niche differentiation of western lake Erie cyanobacterial populations revealed via metatranscriptomic surveys. Environmental Science & Technology 50, 604-615.

12. Paerl, H.W., Otten, T.G., 2016. Duelling 'CyanoHABs': unravelling the environmental drivers controlling dominance and succession among diazotrophic and non-N_2-fixing harmful cyanobacteria. Environmental Microbiology 18, 316-324.

13. Song, H., Lavoie, M., Fan, X., Tan, H., Liu, G., Xu, P., Fu, Z., Paerl, H.W., Qian, H., 2017a. Allelopathic interactions of linoleic acid and nitric oxide increase the competitive ability of *Microcystis aeruginosa*. ISME Journal 11, 1865-1876.

14. Liu, G., Ke, M., Fan, X., Zhang, M., Zhu, Y., Lu, T., Sun, L., Qian, H., 2018. Reproductive and endocrine-disrupting toxicity of *Microcystis aeruginosa* in female zebrafish. Chemosphere 192, 289-296.

15. Qian, H., Zhang, M., Liu, G., Lu, T., Sun, L., Pan, X., 2018b. Effects of different concentrations of *Microcystis aeruginosa* on the intestinal microbiota and immunity of zebrafish (*Danio rerio*). Chemosphere 214, 579-586.

552 16. Qian, H., Xu, J., Lu, T., Zhang, Q., Qu, Q., Yang, Z., Pan, X., 2018a. Responses of
553 unicellular alga *Chlorella pyrenoidosa* to allelochemical linoleic acid. Science of
554 the Total Environment 625, 1415-1422.
555 17. Liu, L., Chen, H., Liu, M., Yang, J.R., Xiao, P., Wilkinson, M., Yang, J., 2019.
556 Response of the eukaryotic plankton community to the cyanobacterial biomass
557 cycle over 6 years in two subtropical reservoirs. ISME Journal 13,
558 doi.org/10.1038/s41396-019-0417-9.
559 18. Liu, M., Liu, L., Chen, H., Zheng, Y., Yang, J.R., Xue, Y., Huang, B., Yang,
560 J.,2019. Community dynamics of free-living and particle-attached bacteria
561 following a reservoir *Microcystis* bloom. Science of the Total Environment 660,
562 501-511.
563 19. Tang, X., Gao, G., Chao, J., Wang, X., Zhu, G., Qin, B., 2010. Dynamics of
564 organic-aggregate-associated bacterial communities and related environmental
565 factors in Lake Taihu, a large eutrophic shallow lake in China. Limnology and
566 Oceanography 55, 469-480.
567 20. Wilhelm, S.W., Farnsley, S.E., Lecleir, G.R., Layton, A.C., Satchwell, M.F.,
568 Debruyn, J.M., Boyer, G.L., Zhu, G., Paerl, H.W., 2011. The relationships
569 between nutrients, cyanobacterial toxins and the microbial community in Taihu
570 (Lake Tai), China. Harmful Algae 10, 207-215.
571 21. Ullah, H., Nagelkerken, I., Goldenberg, S.U., Fordham, D.A., 2018. Climate
572 change could drive marine food web collapse through altered trophic flows and
573 cyanobacterial proliferation. PloS Biology 16, e2003446.

574 22. DeMott, W. R., Gulati, R. D., Van Donk, E., 2001. Daphnia food limitation in
575 three hypereutrophic Dutch lakes: evidence for exclusion of large-bodied species
576 by interfering filaments of cyanobacteria. Limnology and Oceanography 46,
577 2054-2060.
578 23. Paerl, H.W., 1988. Nuisance phytoplankton blooms in coastal, estuarine, and
579 inland waters. Limnology and Oceanography 33, 823-847.
580 24. Brauer, V.S, Stomp, M, Bouvier, T, Fouilland, E, Leboulanger, C, Confurius-Guns,
581 V, Weissing, F.J, Stal, L, Huisman, J., 2015. Competition and facilitation between
582 the marine nitrogen-fixing cyanobacterium Cyanothece and its associated
583 bacterial community. Frontiers in Microbiology 5, 795.
584 25. Hmelo, L.R., van Mooy, B.A.S., Mincer, R. J., 2012. Characterization of bacterial
585 epibionts on the cyanobacterium *Trichodesmium*. Aquatic Microbial Ecology 67,
586 1-14.
587 26. de Figueiredo, D.R., Reboleira, ASSP., Antunes, S.C., Abrantes, N., Azeiteiro, U.,
588 Goncalves, F., Pereira, M.J., 2006. The effect of environmental parameters and
589 cyanobacterial blooms on phytoplankton dynamics of a Portuguese temperate
590 lake. Hydrobiologia 568, 145-157.
591 27. Jones, B.I., 1987. Lake Okeechobee eutrophication research and management.
592 Aquatics 9, 21-26.
593 28. Lu, T., Zhu, Y., Ke, M., Peijnenburg, W.J.G.M., Zhang, M., Wang, T., Chen, J.,
594 Qian, H., 2019. Evaluation of the taxonomic and functional variation of
595 freshwater plankton communities induced by trace amounts of the antibiotic

ciprofloxacin. Environment International 126, 268-278.

29. Klase, G., Lee, S., Liang, S., Kim, J., Zo, Y.G., Lee, J., 2019. The microbiome and antibiotic resistance in integrated fishfarm water: Implications of environmental public health. Science of The Total Environment 649, 1491-1501.

30. Sebastian, M., Ammerman, J.W., 2009. The alkaline phosphatase PhoX is more widely distributed in marine bacteria than the classical PhoA. ISME Journal 3, 563-572.

31. Paerl, H.W. and Millie, D.F., 1996. Physiological ecology of toxic cyanobacteria. Phycologia 35, 160-167.

32. Sukenik, A., Quesada, A., Salmaso, N., 2015. Global expansion of toxic and non-toxic cyanobacteria: effect on ecosystem functioning. Biodiversity and Conservation 24, 889-908.

33. Qian, H., Zhu, Y., Chen, S., Jin, Y., Lavoie, M., Ke, M., Fu, Z., 2018c. Interacting effect of diclofop-methyl on the rice rhizosphere microbiome and denitrification. Pesticide Biochemistry and Physiology 146, 90-96.

34. Te, S.H., Tan, B.F., Thompson, J.R., Gin, K.Y., 2017. Relationship of microbiota and cyanobacterial secondary metabolites in planktothricoides-dominated bloom. Environmental Science & Technology 51, 4199-4209.

35. Haraldsson, M., Gerphagnon, M., Bazin, P., Colombet, J., Tecchio, S., Sime-Ngando, T., Niquil, N., 2018. Microbial parasites make cyanobacteria blooms less of a trophic dead end than commonly assumed. ISME Journal 12, 1008-1020.

618 36. Xue, Y., Chen, H., Yang, J.R., Liu, M., Huang, B., Yang, J., 2018. Distinct patterns
619 and processes of abundant and rare eukaryotic plankton communities following a
620 reservoir cyanobacterial bloom. ISME Journal 12, 2263-2277.
621 37. Zhang, H.L., Du, W.C., Peralta-Videa, J.R., Gardea-Torresdey, J.L., White, J.C.,
622 Keller, A., Guo, H.Y., Ji, R., Zhao, L.J., 2018. Metabolomics reveals how
623 cucumber (*Cucumis sativus*) reprograms metabolites to cope with silver ions and
624 silver nanoparticle-induced oxidative stress. Environmental Science &
625 Technology 52, 8016-8026.
626 38. Welkie, D.G., Rubin, B.E., Diamond, S., Hood, R.D., Savage, D.F., Golden, S.S.,
627 2019. A hard day's night: cyanobacteria in diel cycles. Trends in Microbiology 27,
628 231-242.
629 39. Stincone A., Prigione A., Cramer, M.M.T., Wamelink, K. Campbell, E. Cheung, V.
630 Olin-Sandoval, Grüning, A. N., Krüger, M. Tauqeer Alam., 2014. The return of
631 metabolism: biochemistry and physiology of the pentose phosphate pathway.
632 Biological Reviews 90, 927-963.
633 40. Zhao, L., Huang, Y., Adeleye, A.S., Keller, A.A., 2017. Metabolomics reveals
634 $Cu(OH)_2$ nanopesticide-activated anti-oxidative pathways and decreased
635 beneficial antioxidants in spinach leaves. Environmental Science & Technology
636 51, 10184-10194.
637 41. Zhang, H., Zhao, Z., Kang, P., Wang, Y., Feng, J., Jia, J., Zhang, Z., 2018a.
638 Biological nitrogen removal and metabolic characteristics of a novel aerobic
639 denitrifying fungus *Hanseniaspora uvarum* strain KPL108. Bioresource

Technology 267, 569-577.

42. Zhang, H., Du, W., Peralta-Videa, J., Gardea-Torresdey, J., White, J., Keller, A., Guo, H., Ji, R., Zhao, L., 2018b. Metabolomics reveals how cucumber (*Cucumis sativus*) reprograms metabolites to cope with silver ions and silver nanoparticle-induced oxidative stress. Environmental Science & Technology 52, 8016-8026.

43. Tanabe, Y., Hodoki, Y., Sano, T., Tada, K., Watanabe, M.M., 2018, Adaptation of the Freshwater bloom-forming cyanobacterium *Microcystis aeruginosa* to brackish water is driven by recent horizontal transfer of sucrose genes. Frontiers in Microbiology 9, 1150.

44. Zhao, L., Huang, Y., Paglia, K., Vaniya, A., Wancewicz, B., Keller, A.A., 2018. Metabolomics reveals the molecular mechanisms of copper induced cucumber leaf (*Cucumis sativus*) senescence. Environmental Science & Technology 52, 7092-7100.

45. Waal, D.B.V.D., Ferreruela, G., Tonk, L., Donk, E.V., Huisman, J., Visser, P.M., Matthijs, H.C.P., 2010. Pulsed nitrogen supply induces dynamic changes in the amino acid composition and microcystin production of the harmful cyanobacterium *Planktothrix agardhii*. FEMS Microbiology Ecology, 74, 430-438.

46. Hartmann, J., Albert. A., Ganzera, M., 2015. Effects of elevated ultraviolet radiation on primary metabolites in selected alpine algae and cyanobacteria. Journal of Photochemistry and Photobiology B: Biology 149, 149-155.

662 47. Dai, R., Liu, H., Qu, J., Zhao, X., Hou, Y., 2009. Effects of amino acids on
663 microcystin production of the *Microcystis aeruginosa*. Journal of Hazardous
664 Materials 161, 730-736.
665 48. Cao, D.D., Zhang, C.P., Zhou, K., Jiang, Y.L., Tan, X.F., Xie, J., Ren, Y.M., Chen,
666 Y., Zhou, C.Z., Hou, W.T., 2019. Structural insights into the catalysis and
667 substrate specificity of cyanobacterial aspartate racemase McyF. Biochemical
668 and Biophysical Research Communications 514, 1108-1114.
669 49. GanemQuintanar, A., QuintanarGuerrero, D., Buri, P., 2000. Monoolein: A review
670 of the pharmaceutical applications. Drug Development and Industrial Pharmacy
671 26, 809-820.
672 50. da Silva, G.P., Mack, M., Contiero, J., 2009. Glycerol: a promising and abundant
673 carbon source for industrial microbiology. Biotechnology Advances 27, 30-39.
674 51. Yvonne, Z., Jan-Christoph, K., Sven, M., Keishi, I., Stefan, M., Martin, H., Aaron,
675 K., Thomas, B.R., Elke, D., 2011. The cyanobacterial hepatotoxin microcystin
676 binds to proteins and increases the fitness of microcystis under oxidative stress
677 conditions. PLoS One 6, e17615.
678 52. Poulsonellestad, K.L., Jones, C. M., Roy, J., Viant, M. R., Fernández, F. M.,
679 Kubanek, J., Nunn, B.L., 2014. Metabolomics and proteomics reveal impacts of
680 chemically mediated competition on marine plankton. Proceedings of the
681 National Academy of Sciences USA 111, 9009-9014.
682 53. Song, H., Xu, J., Lavoie, M., Fan, X., Liu, G., Sun, L., Fu, Z., Qian, H., 2017b.
683 Biological and chemical factors driving the temporal distribution of

684 cyanobacteria and heterotrophic bacteria in a eutrophic lake (West Lake, China).
685 Applied Microbiology and Biotechnology 101, 1685-1696.
686 54. Fan, X., Xu, J., Lavoie, M., Peijnenburg, W., Zhu, Y., Lu, T., Fu, Z., Zhu, T., Qian,
687 H., 2018. Multiwall carbon nanotubes modulate paraquat toxicity in *Arabidopsis*
688 *thaliana*. Environmental Pollution 233, 633-641.
689

690 **Tables and Figures**

691 **Table Legends**

692 Table 1 16S Alpha diversity in prokaryotic communities after 4 and 8 d of coculture
693 (Treat-AM4 and Treat-AM8) and monoculture (Con-AM4 and Con-AM4). Different
694 letters represent significant differences within one index ($p < 0.05$). n = 3

695

696 Table 2 18S Alpha diversity in eukaryotic communities after 4 and 8 d of coculture
697 (Treat-AM4 and Treat-AM8) and monoculture (Con-AM4 and Con-AM4). Different
698 letters represent significant differences within one index ($p < 0.05$). n = 3

699

700 Table 3 Metabolic profile changes in culture medium samples of microcosms. VIP
701 represents variable importance.

702

703 **Figure Legends**

704 Figure 1 Design of the experiment and the growth tendency of *M. aeruginosa* and
705 aquatic microorganisms in monoculture and coculture. (A) Experimental flow chart.
706 (B) Optical density (OD_{680}) and cell number of *M. aeruginosa*. (C) Optical density
707 (OD_{680}) and chlorophyll a (Chl-a) of aquatic microcosms. *, ** and *** represent
708 statistically significant differences compared with the control ($p < 0.05$, 0.01 and
709 0.001, respectively). n = 3.
710
711 Figure 2 Water quality parameters of monocultures and cocultures in *M. aeruginosa*
712 and aquatic microcosms. (A, B) Electrical conductivity, (C, D) dissolved oxygen
713 concentrations, and (E, F) pH in *M. aeruginosa* and aquatic microcosms. *, ** and
714 *** represent statistically significant differences compared with the control ($p < 0.05$,
715 0.01 and 0.001, respectively). n = 3.
716
717 Figure 3 (A) Changes in total phosphorus (TP) and inorganic phosphorus (IP) in
718 culture medium. (B) Changes in the nitrate nitrogen ($NO3^-$-N) concentration in culture
719 medium. (C) Changes in the alkaline phosphatase (AKP) concentration in *Microcystis*
720 *aeruginosa* cells. *, ** and *** represent statistically significant differences compared
721 with the control ($p < 0.05$, 0.01 and 0.001, respectively). (D) Changes in the
722 microcystin (MC) concentration in culture medium. n = 3.
723
724 Figure 4 (A) Relative abundance of the 16S rRNA gene of the PCoA plot and (B)

725 RDA ordination diagram of the data, with environmental variables represented by
726 arrows and samples represented by different colors. (C) The main prokaryotic class of
727 the bacterial communities after 4 and 8 d of coculture (Treat-AM4 and Treat-AM8)
728 and monoculture (Con-AM4 and Con-AM8). (D) Top four genera of abundance in
729 *Cyanobacteria* after 4 and 8 d of coculture (Treat-AM4 and Treat-AM8) and
730 monoculture (Con-AM4 and Con-AM8) in aquatic microcosms. Each group had three
731 biological replicates.
732
733 Figure 5 (A) Relative abundance of the 18S rRNA gene of PCoA plot and (B) main
734 eukaryotic phylum of the microbial communities after 4 and 8 d of coculture
735 (Treat-AM4 and Treat-AM8) and monoculture (Con-AM4 and Con-AM8). (C)
736 Scattered atlas of rare microorganisms (Taxonomy represent rare microorganism
737 species). The figure is symmetric along the diagonal, and each dot in the graph
738 represents a rare microbial genus. The first row and the first column represent the
739 distribution of rare microorganisms. The genus near the axis has the lowest relative
740 abundance. The remaining rows or columns represent the comparison between the
741 two groups. Each group had three biological replicates.
742
743 Figure 6 (A) Principal component analysis (PCA) of intracellular *M. aeruginosa*
744 metabolites, cellular microorganisms and culture medium after 8 d of coculture and
745 monoculture. (B) Schematic diagram of proposed metabolic pathways in cellular *M.*
746 *aeruginosa* metabolites and (C) cellular microorganisms after 8 d of coculture and

747 monoculture. Red and green represent up- and downregulated metabolites,
748 respectively. Each group had six biological replicates. PR: photorespiration; PS:
749 photosynthesis.
750
751 Figure 7 Content of Chl-a in aquatic microcosms with monoculture exposed to (a)
752 0-10 μg/L microcystin and (b) 0-2 mg/L D-glyceric acid for different periods of time.
753
754 Figure 8 Schematic diagram of changes in *M. aeruginosa* and microbial communities
755 after coculture treatment. The red color represents upregulation of the metabolites in
756 the treatment group compared to that in the control group, and blue and green colors
757 represent downregulation of metabolites.
758

759 Table 1 16S Alpha diversity in prokaryotic communities after 4 and 8 d of coculture
760 (Treat-AM4 and Treat-AM8) and monoculture (Con-AM4 and Con-AM4). Different
761 letters represent significant differences within one index ($p < 0.05$). n = 3

Sample	Observed species	Shannon	Simpson	ACE	Chao 1	Goods coverage
Con-AM4	303±25^{a}	3.11±0.08^{ab}	0.71±0.01^{ab}	393±25^{a}	396±27^{a}	0.99±0.00^{a}
Treat-AM4	282±52^{ab}	3.19±0.23^{a}	0.73±0.02^{a}	353±64^{a}	360±64^{a}	0.99±0.00^{a}
Con-AM8	247±25^{ab}	2.80±0.04^{ab}	0.65±0.01^{ab}	323±37^{a}	319±30^{a}	0.99±0.00^{a}
Treat-AM8	197±10^{b}	2.55±0.27^{b}	0.63±0.05^{b}	306±7^{a}	297±18^{a}	0.99±0.00^{a}

762

763 Table 2 18S Alpha diversity in eukaryotic communities after 4 and 8 d of coculture

764 (Treat-AM4 and Treat-AM8) and monoculture (Con-AM4 and Con-AM4). Different

765 letters represent significant differences within one index (p< 0.05). n = 3

Sample	Observed species	Shannon	Simpson	ACE	Chao 1	Goods coverage
Con-AM4	46±1^{a}	2.28±0.03^{a}	0.76±0.00^{a}	56±4^{a}	396±27^{a}	0.99±0.00^{a}
Treat-AM4	25±1^{b}	1.98±0.04^{b}	0.68±0.01^{bd}	29±2^{bc}	360±64^{a}	0.99±0.00^{a}
Con-AM8	34±4^{c}	2.14±0.04^{c}	0.71±0.01^{c}	39±4^{b}	319±30^{a}	0.99±0.00^{a}
Treat-AM8	26±2^{bc}	1.77±0.04^{d}	0.67±0.01^{bd}	28±1^{c}	297±18^{a}	0.99±0.00^{a}

766

767 Table 3 Metabolic profile changes in culture medium samples of microcosms. VIP

768 represents variable importance.

Up or down regulation	Candidate metabolite	VIP value	Fold change	P value
▲	Phenaceturic acid	1.00448	∞	3.12E-05
▲	Monoolein	1.03266	∞	4.73E-06
▲	3,6-Anhydro-D-galactose	1.05576	∞	6.23E-07
▲	Dihydroxyacetone	1.06905	∞	8.77E-08
▲	D-Glyceric acid	1.06959	∞	8.71E-08

769

▲	L-Threose	1.07709	∞	1.34E-08
▲	Fucose	1.08395	∞	1.86E-09
▲	Thymidine	1.09358	∞	9.58E-13
▲	Diglycerol	1.09455	∞	1.38E-13
▲	Glycerol	1.09643	11.02	4.84E-18

770

771

772 Figure 1

773

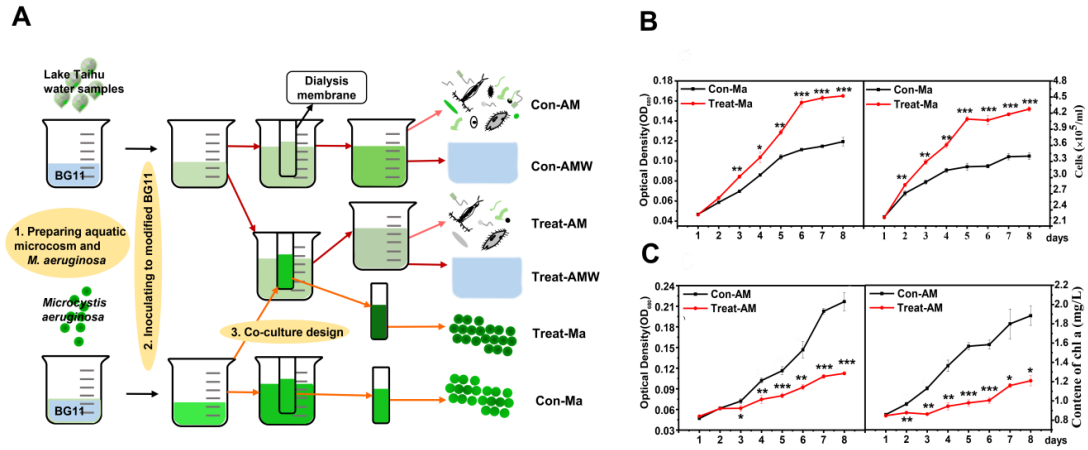

774

775

776 Figure 2

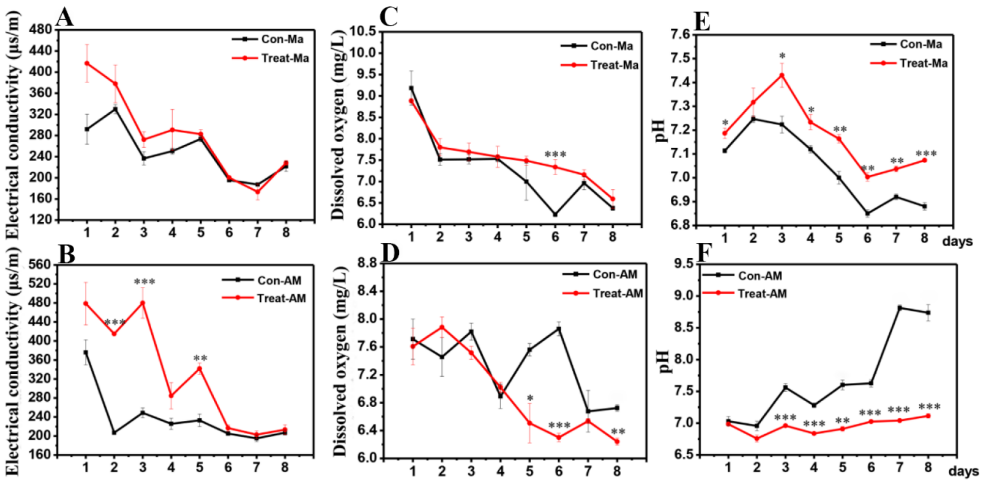

777

778

779

780 Figure 3

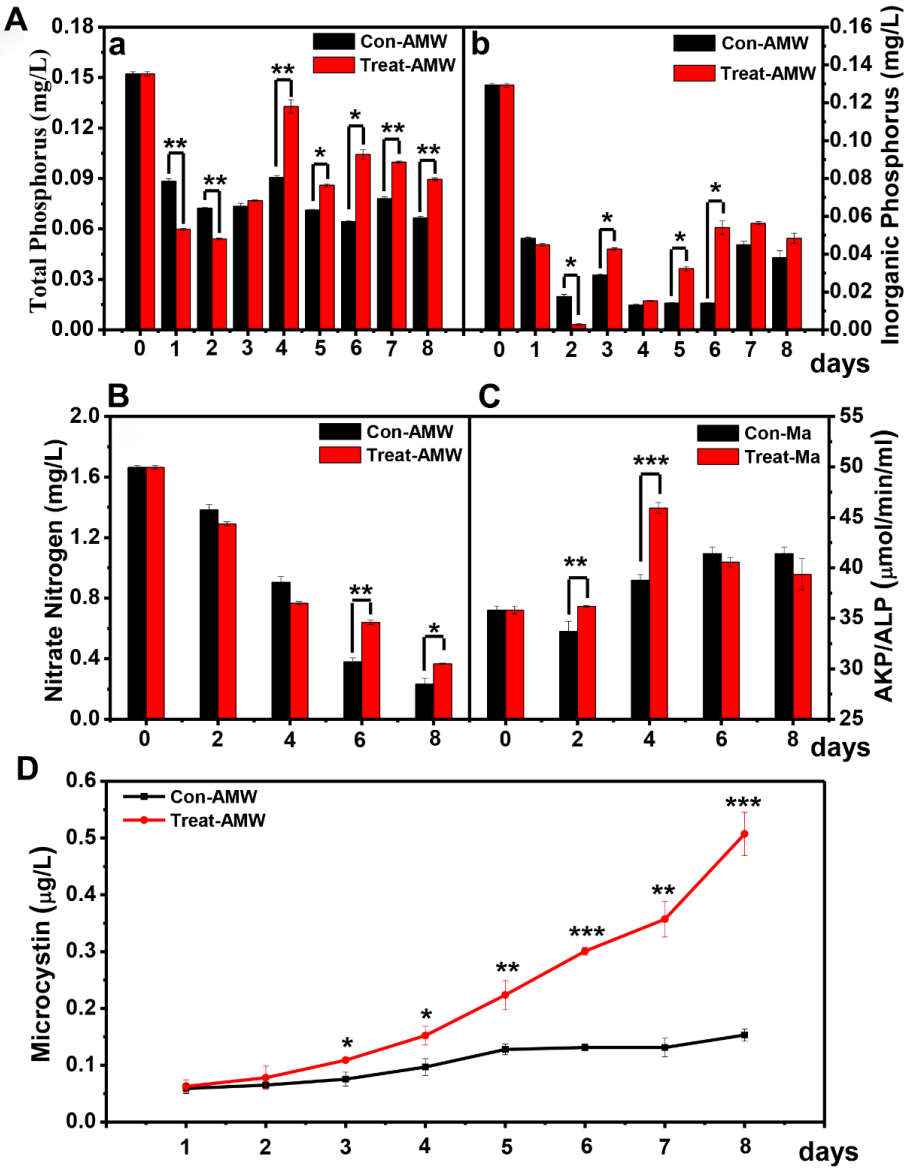

781
782
783

784 Figure 4

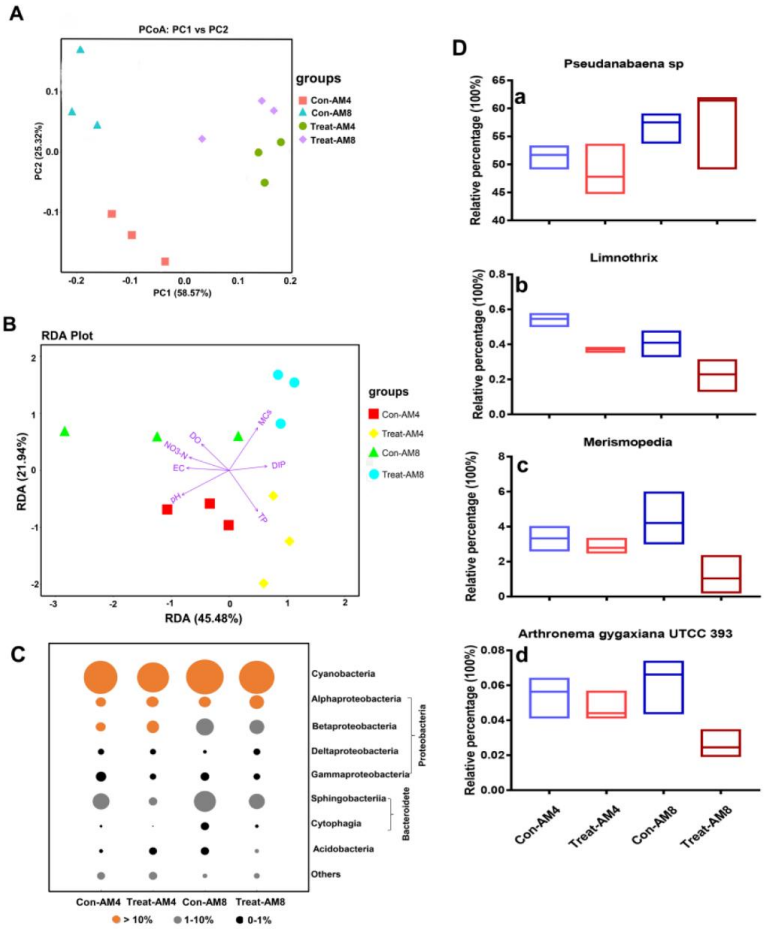

785
786

787

788 Figure 5

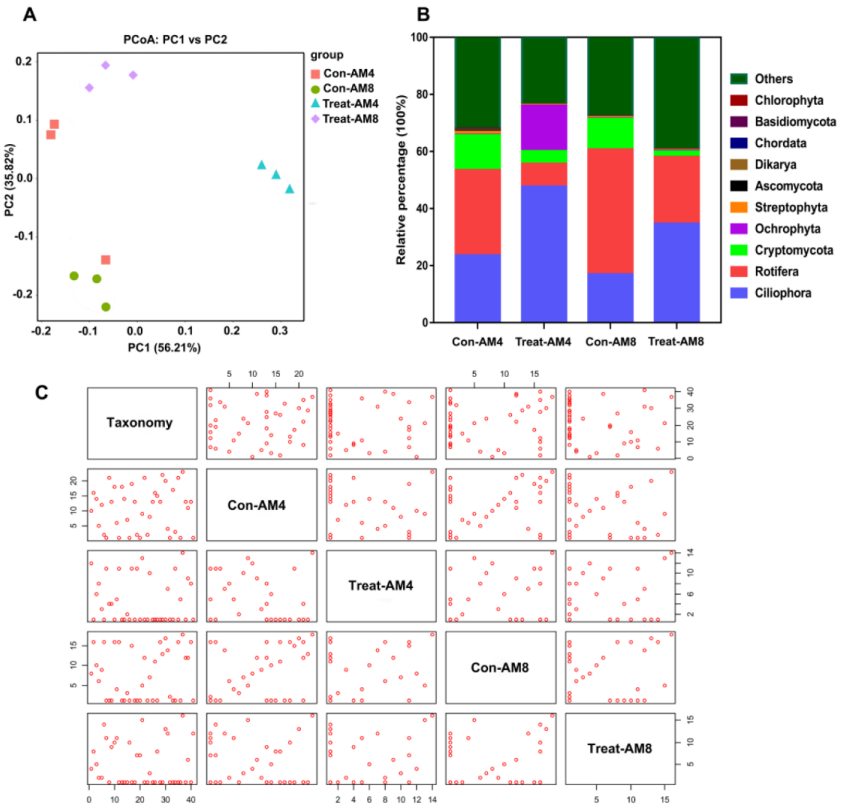

789

790

791 Figure 6

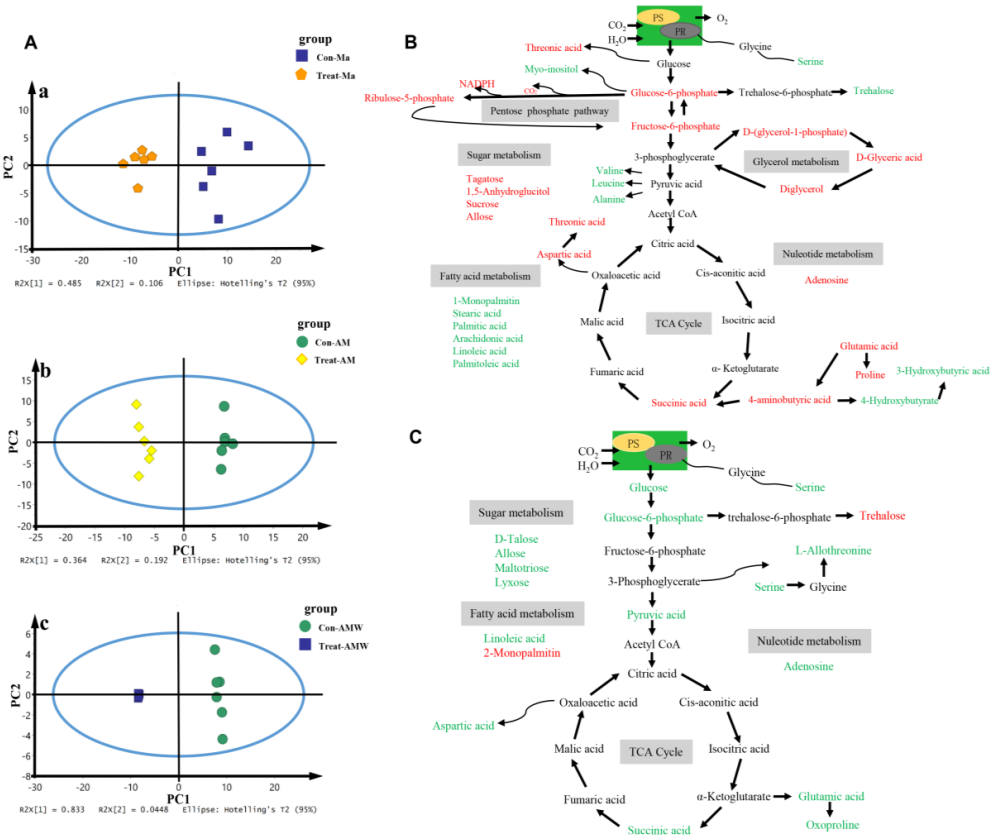

792

793

794 Figure 7

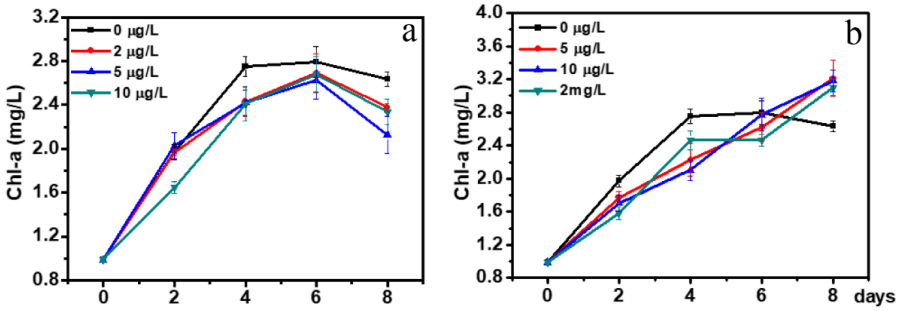

795
796
797

798 Figure 8

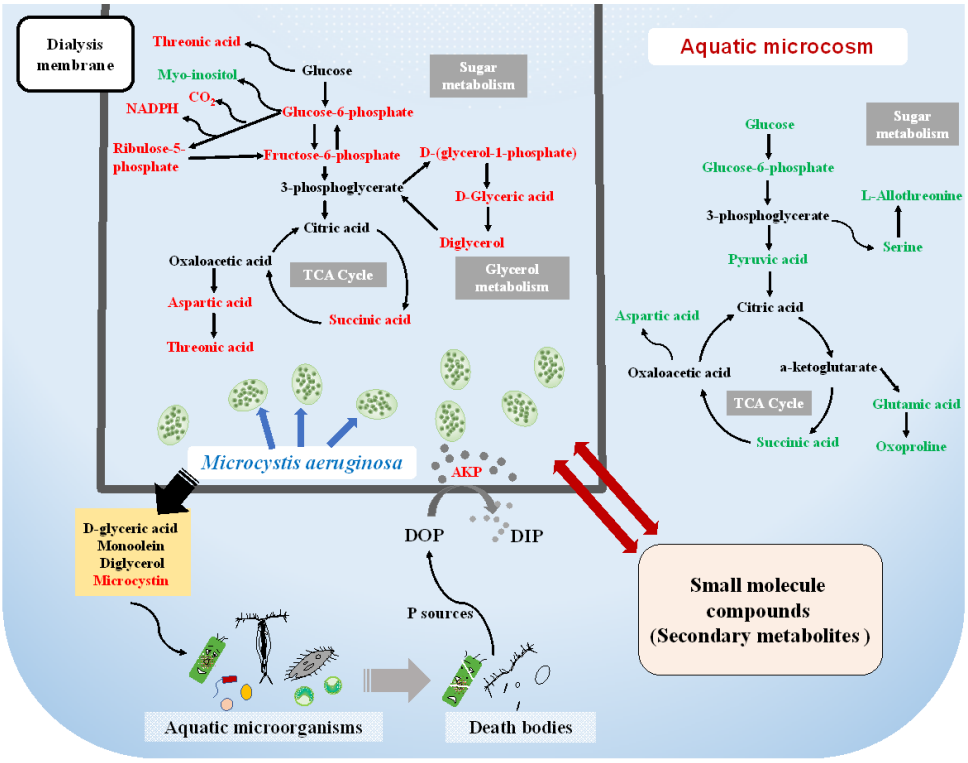

799

800